Proc. NIPR Symp. Polar Meteorol. Glaciol., **8**, 53–65, 1994

THE RELATIONSHIP BETWEEN THE THERMAL BELT ON THE SLOPE OF THE ICE SHEET ON THE SÔYA COAST AND THE SURFACE INVERSION LAYER OVER SYOWA STATION

Kiyotaka NAKAGAWA and Hiroko SHIMODOORI

Division of Science, Joetsu University of Education, Yamayashiki-machi, Joetsu 943

Abstract: All the NOAA/AVHRR thermal infrared images received at Syowa Station from February 1990 to January 1991 were analyzed to make temperature distribution maps. From this analysis the warmer area in midslope, *i.e.* the so-called thermal belt (D. GREENLAND, The Encyclopedia of Climatology, ed. by OLIVER and FAIRBRIDGE, 594, 1987), appeared on the ice sheet slope along the coast around Lützow-Holm Bay, especially on the Sôya Coast, frequently in winter. The relationship between the thermal belt on the Sôya Coast and the surface inversion layer over Syowa Station was investigated. When the surface inversion layer thickness increased, the thermal belt was displaced toward the interior or higher part of the ice sheet slope. However, even if the surface inversion layer appeared over Syowa Staton, the thermal belt did not necessarily appear. The appearance or absence of the thermal belt on the ice sheet slope is considered to correspond to how the surface inversion layer over the ice sheet, a katabatic wind, connects with the surface inversion layer over the foot of the slope.

1. Introduction

The Japanese Antarctic Research Expeditions (JARE) have carried out many oversnow traverse observations on many kinds of glaciological and meteorological subjects on the Mizuho Plateau of the ice sheet near Syowa Station (69°00′S, 39° 35′E). Based upon these observational results, the general view of the temperature distribution in this region becomes clear. It was also discovered that the lapse rate of the ice sheet surface temperature is larger than the dry adiabatic lapse rate (*e.g.* SATOW, 1978; INOUE, 1991). However, since these results were obtained from traverse observations, the data are instantaneous and isolated both in time and in space, and the accuracy is not good.

Recently the utilization of NOAA satellite data has been possible in this region. The data should be directly read at Syowa Station. The advanced very high resolution radiometer on board the NOAA polar orbiting satellite (NOAA/AVHRR) is a scanning radiometer which has five channels (numbered 1–5) in the visible, near infrared, reflected infrared, and thermal, emitted infrared portions of the electromagnetic spectrum (1: 0.58–0.68 μm, 2: 0.725–1.10 μm, 3: 3.55–3.93 μm, 4: 10.3–11.3 μm, 5: 11.5–12.5 μm). Its resolution at the satellite subpoint is 1.1 km. JARE have been receiving the NOAA/AVHRR data at Syowa Station continuously since 1980. The data were corrected to give albedo

or brightness temperature and were mapped on four kinds of grids which were prepared for different purposes (TAKABE and YAMANOUCHI, 1989). The initial data processing was carried out at Syowa Station by JARE immediately after the data were received. The mapped data were stored on computer compatible tapes (CCT) which were later brought back to the National Institute of Polar Research (NIPR), Japan.

The principal advantage of the NOAA/AVHRR data is that they are plane data on the ice sheet surface, and can be obtained every day with about the same accuracy if the sky is cloudless. The distribution map showing the annual mean surface temperature published by KIKUCHI *et al.* (1992) is the first product from the above NOAA/AVHRR data. It is possible to reproduce the lapse rate of the annual mean surface temperature similar to that reported by SATOW (1978) based upon oversnow traverse observations. However, the satellite images had several problems: low resolution due to high compression, large error of at least 50 km in positioning the data point in the chart, mix of cloud and non-cloud pixels, and so on. As a result, it is not possible to discuss the details of the surface temperature distribution on the ice sheet slope except for the interior region with its gently sloping continental ice sheet.

The purpose of the present study is to analyze the detailed surface temperature distribution in Lützow-Holm Bay and its neighborhood, especially near the coast. So the present study uses the type C map which is made at Syowa Station after receiving the satellite data; it covers the whole area of Lützow-Holm Bay with compression of unity. The grid size is 512 by 512, with each pixel representing an area 1.1 km×1.1 km. The surface temperature of the ice sheet can be obtained either from the channel 4 or 5 infrared images. In the present study, channel 4 images are selected from the data archive in the one year period from February 1990 to January 1991.

2. Typical Thermal Belt on the Ice Sheet Slope

Figure 1 shows an example of the distribution map of surface temperature in this area, analyzed for 1600 LST on May 16, 1990. This figure consists of 416×380 pixels, assigning each a gray scale value from black (−50°C) to white (10°C). Isolines of temperatures −45, −40, −35, −30, −25 and −20°C are drawn. Lützow-Holm Bay is in the central part of the figure, with horizontal dimensions around 100 km×300 km. The bay is completely covered with fast ice with heavy snow cover. The Antarctic continent can be seen east and south of the bay, with the Riiser-Larsen Peninsula to the west. There is an open sea area called Ôtone Lead along the northern edge of the fast ice; the pack ice area extends northward from Ôtone Lead.

Since the freezing temperature of sea water is about −2°C, the pack ice area with some open sea is the warmest area in the study area, whose pixel temperature exceeds −20°C. The fast ice area is cold, especially in the extreme interior of the bay where the temperature is lower than −35°C. Despite the warm water under the sea ice, the temperature of the fast ice surface is very low.

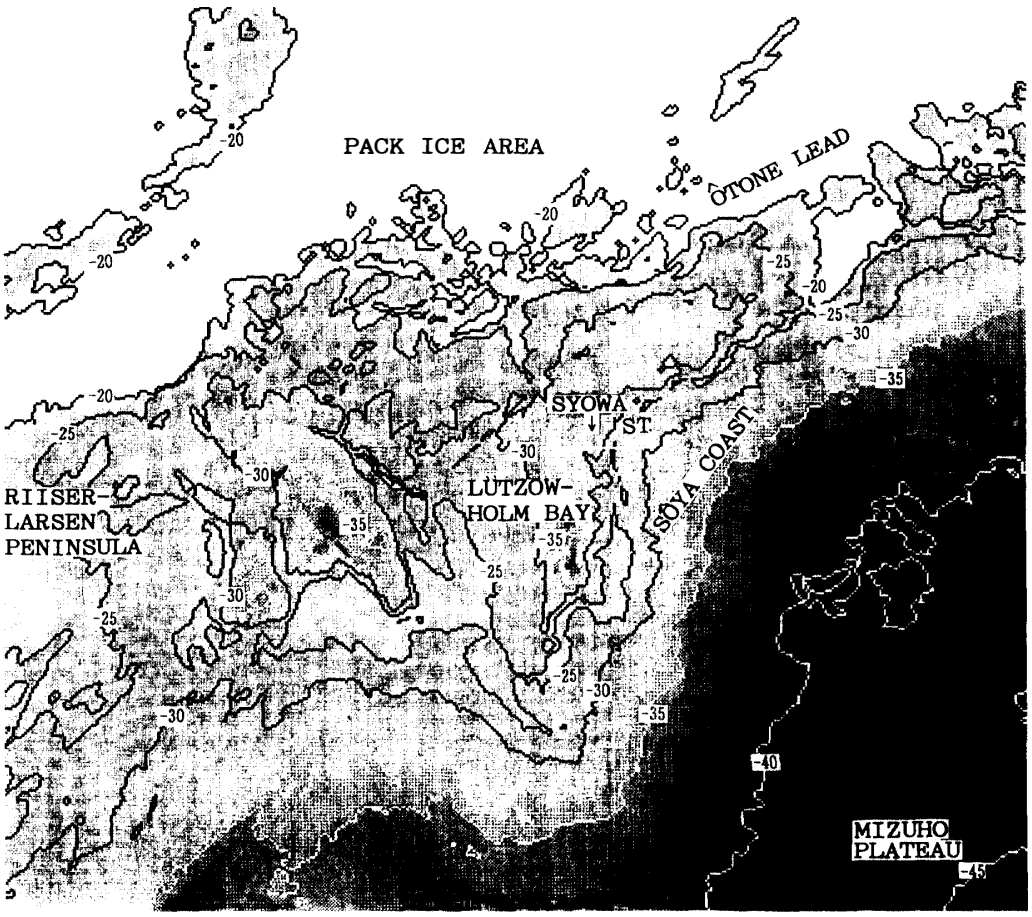

Fig. 1. Example of the surface temperature distribution obtained by NOAA/AVHRR on 1600 LST, May 16, 1990. Isotherms are at 5° intervals. The cross cursor stands for Syowa Station, and the eastward cursor line was used to make the profile of the surface temperature.

This fact suggests that the thick fast ice insulates the heat flow from the underlying sea water to the ice surface, while radiative cooling takes place at the ice surface. However, the ice sheet near the coast of the Antarctic continent is warmer than the fast ice; it is warmer than −25°C in the most of the coastal region. As the altitude of the ice sheet surface increases with departing from the coast, the ice sheet surface temperature decreases; surface temperature isolines run almost parallel to the contour lines. On the Mizuho Plateau, the temperature is lower than −40°C, colder than in the coldest region over the fast ice. There exists a relatively warmer zone along the coast between the fast ice and the interior ice sheet.

The cross cursor in the figure stands for the pixel including the pedestal site of the antenna of Syowa Station in East Ongul Island. As satellite observation time is between 1500 LST and 1700 LST, the observed reflectance from the sunny slope of the ice sheet along the eastward cursor line is higher than that from the flat fast ice over Ongul Strait. Therefore, if we investigate the change of reflectance along the eastward cursor line and identify the point where the

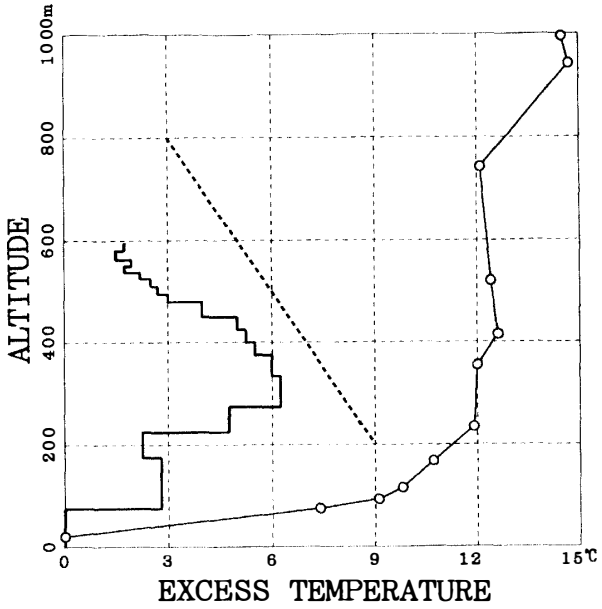

Fig. 2. Comparison of profiles of surface temperature on ice sheet slope (1600 LST) and of the ascending air temperature at Syowa Station (1500 LST). The heavy solid line is the surface temperature profile on the ice sheet slope along the eastward cursor line in Fig. 1, the heavy dotted line is the dry adiabatic lapse rate (=10 K/km), and open circles show the ascending sonde profile at Syowa Station at 1500 LST on May 16, 1990.

rapid increase of reflectance starts, we can easily determine the pixel which includes the coast line. The coast line is located at the fourth pixel eastward from the pixel including the pedestal site of the antenna of Syowa Station. If we investigate the location of the above-mentioned warmer zone, we find that the warmest temperature occurs at land pixels which do not include the coast line.

Figure 2 shows the profile of the surface temperature of ice sheet along the eastward cursor line shown in Fig. 1. The ordinate is altitude, determined from the pixel number based on the contour map of the Sôya Coast region made by JARE. The abscissa is for the excess temperature of the interior pixel from the pixel at the coast line. It is clear that the interior pixels are warmer than the coast pixel, and that the maximum of the excess temperature, about 6.3°, occurs at the fourth pixel from the coast where the altitude is estimated to be about 300 m. Eastward from this point, the surface temperature decreases with altitude. The above feature suggests that there exists a so-called thermal belt on the ice sheet slope in the Antarctic continent near Lützow-Holm Bay, at least in the Sôya Coast region.

3. Annual Change of the Thermal Belt on the Sôya Coast

The satellite image does not necessarily coincide with the geographical map, chiefly because the orbit parameters of the satellite used for making images are

not correct and/or the attitude of the satellite is unknown. Although in principle the disagreement of the image with the map includes the rotation of the image relative to the map, in fact the disagreement consists chiefly of parallel displacement. Therefore, if we can use at least one ground control point (GCP) in the NOAA/AVHRR images, it becomes possible to investigate the temporal change at corresponding pixels among several images.

The present study uses an isolated rock pixel as the GCP in the warm season, because the rock pixel with lower albedo is remarkably warmer than the surrounding ice pixels and is easily identified in the NOAA/AVHRR channel 4 image. However, the rock pixel can not be used as the GCP in winter, because the temperature difference between rock and ice pixels vanishes. The present study uses segments of the fast ice edge with identifiable shape, such as a large scale crack which occurred in the middle of Lützow-Holm Bay in the middle of April before the polar night, as GCP in winter. Even after the crack closed again during the polar night, a clear trace remained on the fast ice surface in the thermal image. The crack trace did not move during the polar night.

In order to investigate the annual change of the thermal belt on the Sôya Coast ice sheet slope, first, we corrected the satellite image positions through a whole year from February 1990 to January 1991. When no GCP can be seen in the satellite image, correction of the position is impossible. Among the 343 available afternoon path images, the positions of 177 were corrected, using the image of December 26, 1990 as the standard image (see Table 1). The present study used 80 images selected from these corrected images, in which the Sôya Coast ice sheet slope was not covered by cloud.

Figure 3 shows the annual march of the pixel number of the warmest pixel on the slope from the coast along the eastward cursor shown in Fig. 1. The pixel number corresponds to the location or height of the thermal belt. It is clear from this figure that the thermal belt appears more frequently in winter, and that the

Table 1. Monthly summary of position correction of NOAA11/AVHRR images received by JARE-31 at Syowa Station.

Year	'90											'91	
Month	Feb.	Mar.	Apr.	May	June	July	Aug.	Sep.	Oct.	Nov.	Dec.	Jan.	Total
Received paths	33	33	38	38	29	33	32	39	35	33	33	26	402
Afternoon paths	28	31	30	31	27	31	30	30	31	30	31	13	343
Position corrected scenes	15	10	12	15	17	8	17	23	11	21	22	6	177
GCP of rock	15	10	10	7	9	2	4	17	11	21	22	6	134
GCP of ice			3	10	11	6	14	7					51
GCP of rock and ice			1	2	2			1					6

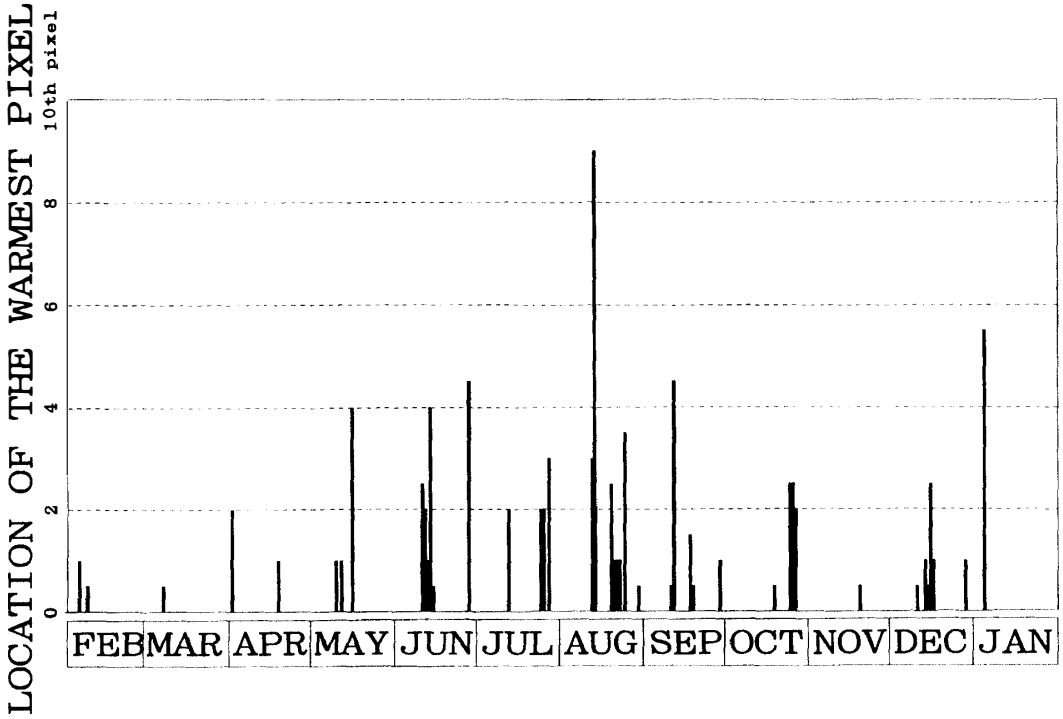

Fig. 3. The annual march of the thermal belt location, the pixel number from the coast of the warmest pixel on the slope along the eastward cursor in Fig. 1, from February 1990 to January 1991.

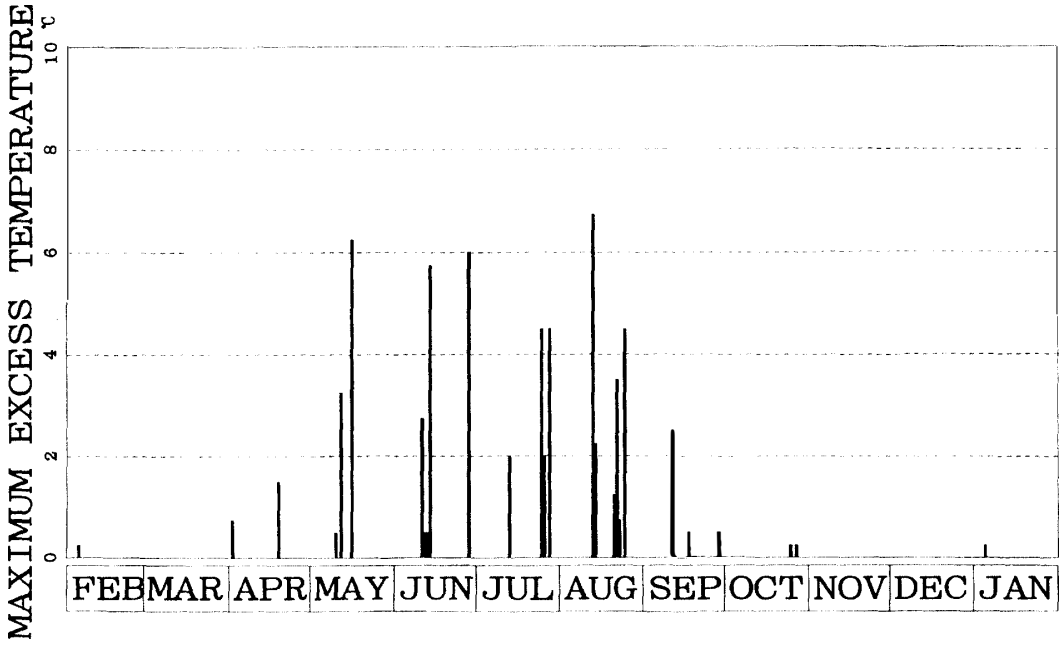

Fig. 4. The annual march of the thermal belt intensity, the excess temperature of the warmest pixel from the coast (same format as Fig. 3).

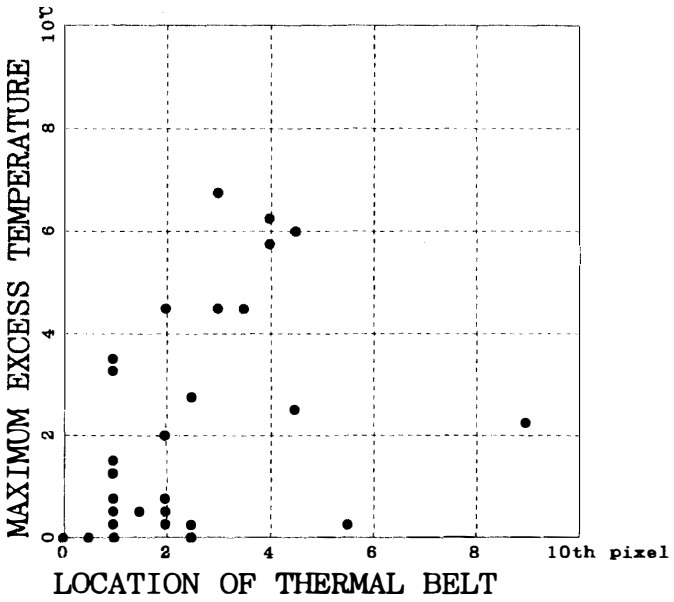

Fig. 5. The plot of location versus intensity of the thermal belts.

warmest pixel appears in the interior, *i.e.* on the higher part of the ice sheet slope, in winter. Most of the thermal belts appear within 5 pixels from the coast; the maximum was 9. However, if there are clouds over the slope, it is impossible to analyze the temperature distribution along the slope. Therefore, we can not conclude only from the above figures that the thermal belt appears only in the cold season.

Figure 4 shows the annual march of the excess temperature of the warmest pixel from the coast pixel. The above excess temperature corresponds to the intensity of the thermal belt. It is clear from Fig. 4 that the strong thermal belt appears more frequently in winter. The excess temperature frequently exceeded 3°C during winter, while such a strong thermal belt did not appear in other seasons.

Figure 5 shows the relationship between the location and the intensity of thermal belts. It is clear from this figure that, when the intensity is stronger, the thermal belt appears higher on the slope.

4. Annual Change of the Surface Inversion Layer over Syowa Station

In Fig. 2, the ascending sonde profile of air temperature at Syowa Station at 1500 LST on May 16, 1990, which was approximately synchronized with the satellite observation, is also plotted. In this profile there exists a strong surface inversion layer with thickness of about 300 m and intensity of more than 10°C. Above the surface inversion layer, there exists another upper level inversion layer due to down draft or advection between 800 m and 1000 m. The altitude of the thermal belt seems to agree well with the top of the surface inversion layer.

Figures 6 and 7 show the annual marches of the thickness and intensity of the surface inversion layer over Syowa Station, as determined from ascending

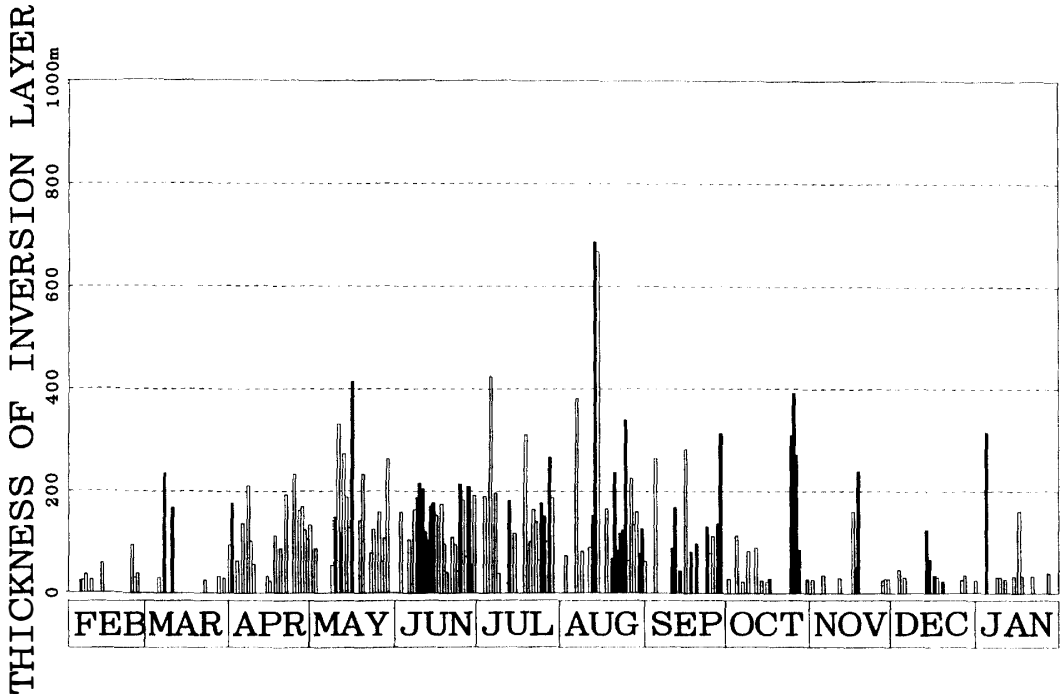

Fig. 6. The annual march of the height of the surface inversion layer over Syowa Station (same format as Fig. 3). Black columns are days when satellite data are available; white columns are other days.

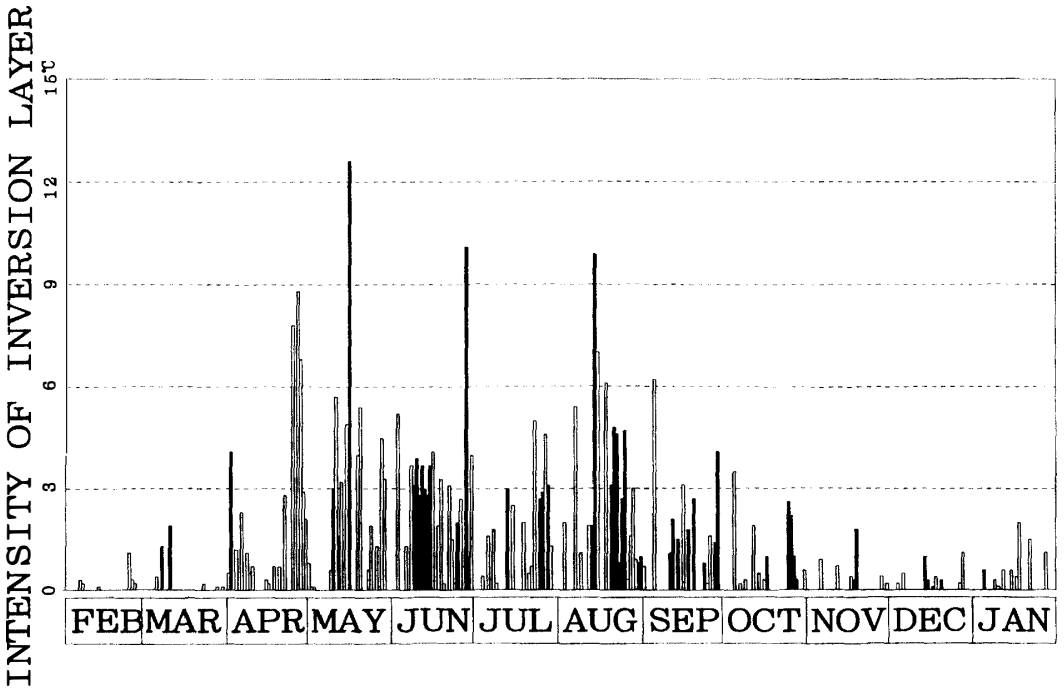

Fig. 7. The annual march of the intensity of the surface inversion layer over Syowa Station (same format as Fig. 6).

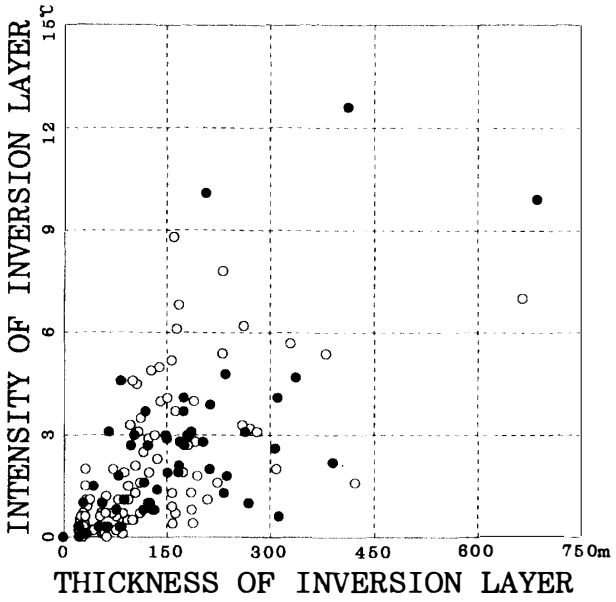

Fig. 8. The plot of thickness versus intensity of the surface inversion layers over Syowa Station. Solid circles are days when satellite data are available; open circles are other days.

temperature profiles at 1500 LST. The thickness and intensity of the inversion layer are determined by the differences of, respectively, heights and temperatures between the top and bottom of the layer. The black columns are on days when surface temperature profiles are available along the ice sheet slope in the satellite image; the white columns are on other days. It is clear from these figures that the surface inversion layer over Syowa Station appears more frequently in winter, and that both height and intensity of the surface inversion layer are also larger in winter. In addition, the annual trends shown in Figs. 6 and 7 are similar to those in Figs. 3 and 4.

Figure 8 shows the relationship between thickness and intensity of the surface inversion layer. There is a linear relation between thickness and intensity of the surface inversion layer. As the thickness of surface inversion layer is larger, the intensity of the surface inversion layer is stronger.

5. The Relationship Between the Thermal Belt and the Surface Inversion Layer

The patterns of scatters of dots shown in Figs. 5 and 8 are similar to each other. This fact suggests that there exists some relationship between the thermal belt on the ice sheet slope and the surface inversion layer over Syowa Station.

Figure 9 shows the relationship between the surface inversion layer thickness and thermal belt location. Thermal belt location 0 means absence of the thermal belt. It is clear from this figure that, even if there is a surface inversion layer over Syowa Station, the thermal belt does not necessarily appear on the ice sheet slope, and that if the thermal belt appears, its location shifts inland with

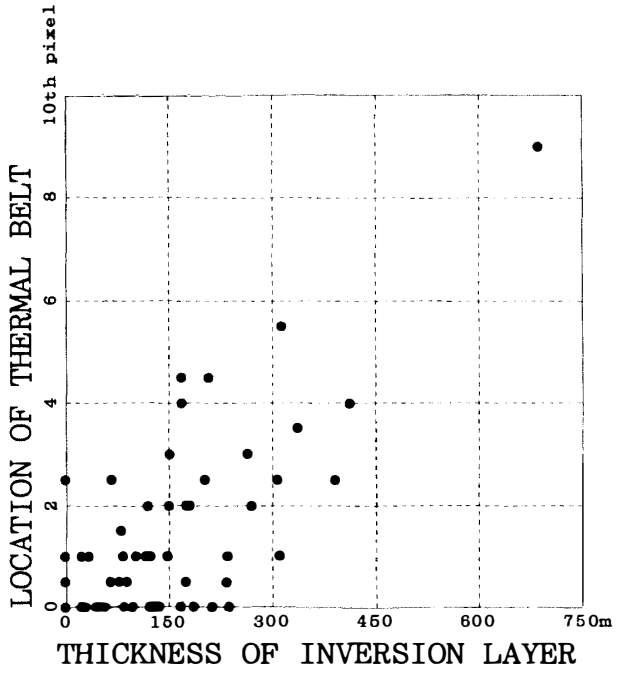

Fig. 9. The plot of the surface inversion layer thickness over Syowa Station versus thermal belt location.

increasing surface inversion layer thickness over Syowa Station.

This fact suggests that the thermal belt results from the interaction between the surface inversion layer over the flat fast ice at the foot of the ice sheet slope and the surface air layer on the slope, *i.e.* the katabatic wind.

6. Discussion: Necessary Condition for Appearance of the Thermal Belt

INOUE (1991) discussed the factors controlling the surface temperature lapse rate on the Antarctic ice sheet, using the following expression for the surface air temperature of the ice sheet in °C, T_s;

$$dT_s = -\beta dy - \gamma (dh + dh_i) - dT_i, \tag{1}$$

where y is the southward distance from the edge of the ice sheet in km, h is the ice sheet surface elevation in km, h_i is the thickness of the surface inversion layer over the ice sheet in km, and β and γ are, respectively, horizontal and vertical gradients of the free atmosphere air temperature, which are almost constants (β=0.04°C/km, γ=5.0°C/km). T_i is the surface inversion layer intensity in °C, and it is a liner function of the surface air temperature as follows;

$$T_i = -AT_s - B, \tag{2}$$

where A and B are experimental coefficients, and their typical values in winter are, respectively, 0.38 and 3.1 (INOUE, 1991). Since eq. (2) was derived statisti-

cally from monthly mean air temperatures observed at all weather stations on the Antarctic ice sheet, it does not necessarily hold at the foot of the ice sheet slope near Syowa Station.

Figure 10 shows the relationship between surface inversion layer intensity and surface air temperature at Syowa Station at 1500 LST on cloudless days from February 1990 to January 1991. The heavy solid line is the regression line proposed by INOUE (1991), and the thin solid line is the regression line derived from plotted data by the least squares method. Although these regression lines are different, the scatter of dots of Fig. 10 in the temperature range from −40°C to 10°C is about the same as that of Fig. 3 of INOUE (1991) derived for the temperature range from −80°C to 10°C. So the present study assumes that eq. (2) holds throughout the ice sheet slope including the foot, and that the surface air temperature on the ice sheet is equal to the ice surface temperature.

In addition, the present study expresses h as a function of y as follows;

$$h=L\{1-\exp(-\tau y)\}, \tag{3}$$

where L (=4.0 km) is the maximum ice sheet elevation and τ (=3.02×10^{-3} km^{-1}) is the polarward extinction coefficient.

After substituting eqs. (2) and (3) into eq. (1), differentiating eq. (1) by a height gives the following formula:

$$\frac{(1-A)}{\gamma}\frac{dT_s}{dh} = -\frac{\beta}{\gamma\tau(L-h)} - 1 - \frac{dh_i}{dh}. \tag{4}$$

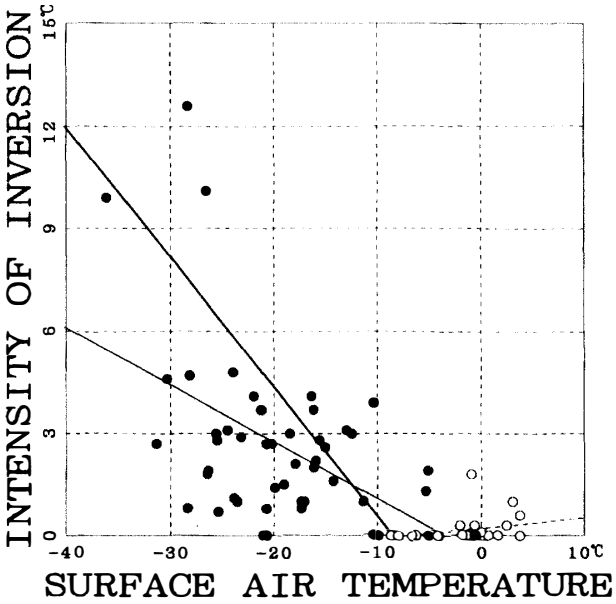

Fig. 10. The plot of surface air temperature versus surface inversion layer intensity at Syowa Station. Solid circles are in winter (March to October); open circles are in summer. Thin solid and dashed lines are the regression lines for, respectively, winter and summer; the heavy solid line is the regression line for winter proposed by INOUE (1991).

In order for the thermal belt to exist, it is necessary to have:

$$\frac{dT_s}{dh} > 0, \tag{5}$$

at least near the sea coast, or $h=0$. Since $1-A>0$, the necessary condition for the appearance of the thermal belt is as follows:

$$-1 > -\frac{\beta}{\gamma\tau L} - 1 > \frac{dh_i}{dh}, \ (h = 0) \tag{6}$$

Equation (6) means that, in order for the thermal belt to appear, it is necessary for the surface inversion layer thickness to decrease more rapidly than the increase in ice sheet surface elevation. When the above necessary condition is satisfied, the thermal belt appears at the altitude where $dT_s/dh=0$.

As mentioned above, even if the surface inversion layer exists over the flat fast ice at the foot of the slope, the thermal belt on the slope appears at sometimes and not others. The authors think that the presence or absence of the thermal belt corresponds to whether the above necessary condition is satisfied or not. Since the surface inversion layer on the ice sheet slope is the katabatic wind for its own sake, the rapid increase in the thickness of the surface inversion layer on the foot of the slope means the rapid increase in the height of the top of the katabatic wind layer. This phenomenon is expected to appear both when the total thickness of the katabatic wind layer increases at the foot of the slope because of a rapid decrease in wind velocity and when the katabatic wind leaves the slope and runs on the surface inversion layer over the foot of the slope like a hydraulic jump because of the smaller density.

7. Concluding Remarks

The present study analyzed the annual march of the surface temperature distribution, on the ice sheet slope at the Sôya Coast with NOAA/AVHRR channel 4 data from February 1990 to January 1991, after the position correction of satellite images using an isolated rock and/or the crack or its trace on fast ice as the GCP. As a result, the present study discovered a thermal belt on the ice sheet slope at the Sôya Coast.

The thermal belt appears frequently in winter. When the thermal belt appears higher on the slope, the excess temperature of the warmest pixel from the coast pixel is larger. As a result of comparing the surface temperature distribution on the slope with the ascending air temperature profile over the foot of the slope, relationships were discovered between the location and excess temperature of the thermal belt and the thickness and intensity of the surface inversion layer over the foot of the slope. Even if there is a surface inversion layer over the foot of the slope, the thermal belt does not necessarily appear on the slope. If the thermal belt appears on the slope, its location is more interior, or higher, with increasing thickness of the surface inversion layer over the foot of the slope.

The present study yielded a necessary condition for the appearance of the thermal belt, based upon INOUE's (1991) formulation, and we believe that the appearance or absence of the thermal belt corresponds strongly with whether the above necessary condition is satisfied or not. However, at the present time, we have little information about the function $h_i=h_i(h)$ near the foot of the ice sheet slope. Therefore, most of our discussion is speculative. Accumulation of information about the interaction between the surface inversion layer at the foot and middle of the ice sheet slope, especially about the function $h_i=h_i(h)$, is needed.

Acknowledgments

One of the authors, Dr. K. NAKAGAWA, wishes to express his sincere thanks to the members of the wintering party of JARE-31 for their kind assistance in receiving and processing the satellite data at Syowa Station. The authors are also grateful to Dr. T. YAMANOUCHI, National Institute of Polar Research, for his useful discussion and comments, and to two anonymous referees for their useful comments in revising this paper.

References

GREENLAND, D. (1987): Mountain climates, upland. The Encyclopedia of Climatology, ed. by J. E. OLIVER and R.W. FAIRBRIDGE. New York, Van Nostrand Reinhold, 594–601 (Encyclopedia of Earth Sciences, Vol. 11).

INOUE, J. (1991): Nankyoku hyôshô-jô no kion o shihaisuru yôin (The factors governing the surface air temperature on the ice sheet of Antarctic Continent). Kôri Koa Kaiseki ni yoru Hyôga Hyôshô no Dôrikigaku-teki Tokusei to Kankyô Hendô ni kansuru Sôgô Kenkyû (The General Study on Dynamic Characteristic and Environment Change of Glacier and Ice Sheet with Ice Core), ed. by G. WAKAHAMA. Sapporo, Hokkaido University, 193–202.

KIKUCHI, T., SATOW, K., OHATA, T., YAMANOUCHI, T. and NISHIO, F. (1992): Wind and temperature regime in Mizuho Plateau, East Antarctica. Int. J. Remote Sensing, **13**, 67–79.

SATOW, K. (1978): Distribution of 10 m snow temperatures in Mizuho Plateau. Mem. Natl Inst. Polar Res., Spec. Issue, **7**, 63–71.

TAKABE, H. and YAMANOUCHI, T. (1989): NOAA data processing system. Nankyoku Shiryô (Antarct. Rec.), **33**, 73–87.

(Received November 26, 1993; Revised manuscript received May 28, 1994)